

Cross-sectional imaging of sharp Si interlayers embedded in gallium arsenide

Xiangmei Duan^{a)}

INFN-DEMOCRITOS National Simulation Center, via Beirut 2-4, 34014 Trieste, Italy

Stefano Baroni

INFN-DEMOCRITOS National Simulation Center, via Beirut 2-4, 34014 Trieste, Italy

and SISSA—Scuola Internazionale Superiore di Studi Avanzati, via Beirut 2-4, 34014 Trieste, Italy

Silvio Modesti

INFN-TASC National Laboratory, Area Science Park, 34012 Trieste, Italy

and Dipartimento di Fisica, Università di Trieste, via Valerio 2, 34127 Trieste, Italy

Maria Peressi^{b)}

INFN-DEMOCRITOS National Simulation Center, via Beirut 2-4, 34014 Trieste, Italy

and Dipartimento di Fisica Teorica, Università di Trieste, Strada Costiera 11, 34014 Trieste, Italy

(Received 29 March 2005; accepted 15 November 2005; published online 13 January 2006)

We investigate the electronic properties of the (110) cross-sectional surface of Si-doped GaAs using first-principles techniques. We focus on doping configurations with an equal concentration of Si impurities in cationic and anionic sites, such as occurring in a self-compensating doping regime. In particular we study a bilayer of Si atoms uniformly distributed over two consecutive (001) atomic layers. The simulated cross-sectional scanning tunneling microscopy images show a bright signal at negative bias, which is strongly attenuated when the bias is reversed. This scenario is consistent with experimental results which had been attributed to hitherto unidentified Si complexes. © 2006 American Institute of Physics. [DOI: 10.1063/1.2162690]

Si-doped GaAs has an outstanding importance in the technology of electronic devices. Remarkably, Si in GaAs has an amphoteric behavior—being able to substitute both arsenic and gallium atoms as an acceptor or a donor, respectively—resulting in a compensation mechanism that depends on the growth conditions and has been long debated.^{1,2} Recently, GaAs samples with Si δ -doped layers embedded in the (001) direction have started to be investigated by cross-sectional scanning tunneling microscopy (XSTM) and spectroscopy on the (110) easy-cleavage surface.^{1,3} It was found that in samples grown at 600 °C, Si self-compensation occurs above a surface Si concentration of about 0.06 monolayer (ML) and involves nucleation and growth of electrically neutral Si precipitates at the expense of the conventional donor Si phase.¹ In the XSTM images of such samples, beside the common and well identified defects such as silicon donors (Si_{Ga}) and gallium vacancies (V_{Ga}), new features appear, bright at negative bias and strongly attenuated when the bias is reversed. The microscopic picture of these features is still unidentified, although it is clear that they cannot be attributed to Si_{Ga} donors only (whose STM images are well characterized and remarkably different) nor to substitutional-vacancy complexes such as $\text{Si}_{\text{Ga}}-\text{V}_{\text{Ga}}$ or $\text{Si}_{\text{Ga}}-\text{V}_{\text{As}}$, as previously proposed.² This kind of contrast is also peculiar to the XSTM image of a bilayer of Si in GaAs, as shown in Fig. 1.

A few theoretical studies of Si-doped or otherwise defected GaAs (110) surfaces exist,⁴⁻⁹ but to the best of our knowledge no attempts have been done so far to model ex-

tended self-compensating donor-acceptor configurations. The purpose of the present paper is to start filling this gap by providing the first theoretical study of XSTM images resulting from the cleavage of (001) Si interlayers embedded in GaAs. When Si substitutes both Ga and As atoms in consecutive GaAs (001) atomic layers, the resulting configuration is self-compensating and corresponds to a *microscopic capacitor* with unique electronic properties.^{10,11} A self-compensating layer configuration is required by electrostatic stability, whereas its confinement and the value of the resulting dipole are limited by atomic interdiffusion. We study the simplest possible configurations, that is, an entire Si (001) bilayer confined onto two adjacent atomic planes and the case of one monolayer uniformly distributed over two such planes. We also study isolated surface donor-acceptor pairs

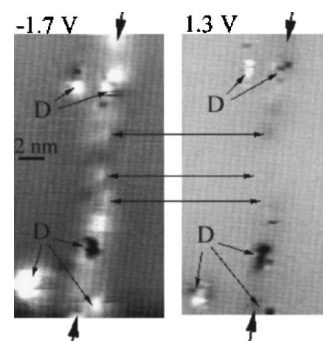


FIG. 1. XSTM images of the same region of the intersection between 2 ML of Si in GaAs parallel to the (001) plane and the (110) cleavage surface taken at a sample bias of -1.7 V (left) and 1.3 V (right). The tunneling current is 0.2 nA. The intersection line is marked by vertical arrows. Horizontal arrows connect corresponding points of the Si layer. D indicates cleavage defects. The Si layer was grown by molecular beam epitaxy at 600 °C and analyzed by XSTM with the methods described in Ref. 1.

^{a)}Present address: School of Physics, The University of Sydney, NSW 2006, Australia.

^{b)}Electronic mail: peressi@ts.infn.it

which can be considered the building blocks of extended self-compensating donor-acceptor configurations. In all the cases, XSTM images have been simulated using the electronic-structure data resulting from our calculations.

The study of cross-sectional surfaces is conceptually similar to that of natural surfaces and can be afforded using supercells with slab geometries.¹² Our numerical approach is based on the plane-wave pseudopotential method in the framework of density functional theory (DFT) within the local-density approximation (LDA), using the ESPRESSO/PWSCF code.¹³

The calculated structural properties of GaAs, bulk and along (110) surface, are of the same good quality as currently found in the literature. The calculated energy gap for bulk GaAs is 1.36 eV, slightly underestimated with respect to the experimental value, as it typically occurs in DFT-LDA calculations. The clean surface is semiconducting, with a calculated energy gap smaller than the bulk value by about 0.5 eV. The surface geometry is optimized by allowing all the atomic position to relax. STM images are obtained with the simple and widely used model by Tersoff and Hamann.¹⁴ According to this model, the tunneling current is proportional to the local density of states (DOS) calculated at the position of the tip and integrated in the energy range between the Fermi energy E_F and $E_F + eV_b$, where V_b is the applied bias. In this model the proximity of the tip is assumed not to perturb the electronic structure of the surface.

The position of the calculated Fermi energy depends sensitively on the concentration of dopants which is contrivedly large, for it depends on the size of the supercell. It is therefore appropriate to use the experimental value of the Fermi energy in order to simulate XSTM images from our calculated electronic-structure data. The experimental samples are overall *n*-doped, and the Fermi energy is thus close to the bottom of the conduction band. Taking into account that our calculated surface gap is approximately 0.3 eV smaller than the experimental value, the experimental data at $V_b = -1.7$ V and $V_b = 1.3$ V have to be compared with our calculations at $V_b \approx -1.5$ V and $V_b \approx 1.2$ V, respectively.

We mainly study neutral configurations. However, in the Si-doped samples that we consider, diffused as well as localized doping together with the presence of the surface may induce some charge accumulation. This may affect band structure and DOS not only by rigidly shifting them with respect to the Fermi energy but also by modifying their shape. For these reasons, we also examine some charged states of the samples and we investigate their effects on the structural and electronic properties in a self-consistent way.

Our tests on the clean (110) surface and with the isolated Si_{Ga} surface substitutional impurity confirm the findings of previous experimental and theoretical investigations,^{2,4} thus validating our approach. We have therefore considered the possible scenarios arising from a progressively higher Si doping of GaAs in the hypothesis of donor configurations (Si_{Ga}) only: two surface Si_{Ga} impurities with different relative positions (on-surface or subsurface) up to an entire row (again on-surface or subsurface) or even an entire monolayer, abrupt or spread over two adjacent cationic planes. The simulated XSTM images for all these configurations—*not shown here*—do not correspond to the bright features at negative bias and attenuated contrast at positive bias observed in the recent experiments: they would rather look the opposite.

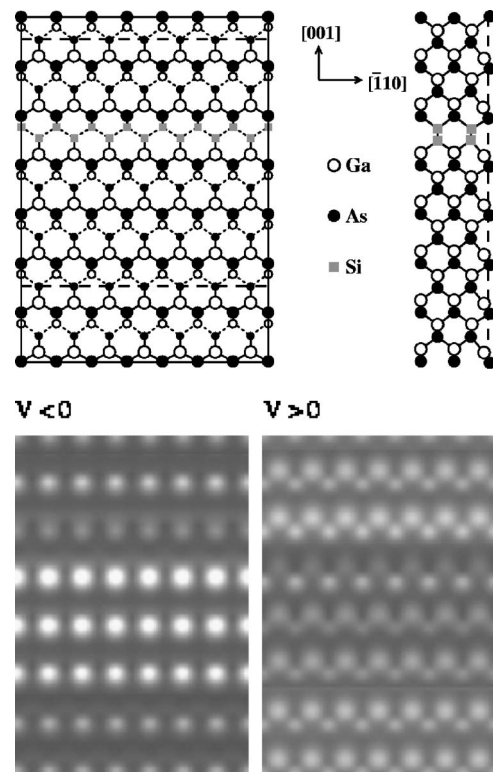


FIG. 2. (001) Si bilayer in GaAs: case with Si_{Ga} and Si_{As} subsurface (case B). Top panels: ball and stick model of the relaxed surface, top and side view (Ga: open circle, As: closed circle, Si: square). Dashed lines in the top view indicate the extension in the [001] direction of the supercell used to simulate the system with the interlayer. In the figure the supercell is repeated in the [110] direction but not in the [001] direction, where it is instead embedded in the perfect clean surface to give a better feel of the image of an isolated interlayer. Right panels: simulated STM images at bias voltages of -1.5 eV (occupied states) and at $+1.2$ eV (empty states), respectively. The size of the entire region shown in our simulated STM images corresponds to $\approx 2.75 \text{ nm} \times 3.89 \text{ nm}$.

We then consider a uniform distribution of substitutional Si_{Ga} and Si_{As} atoms over two adjacent cationic and anionic (001) layers. The intersection of the (110) surface with the Si (001) bilayer can occur in different positions and can thus result in different configurations of the exposed surface that can include rows of Si atoms in As and/or Ga sites. There are four different possible configurations: (A) both Si_{Ga} and Si_{As} on-surface, forming a zigzag chain; (B) both Si_{Ga} and Si_{As} subsurface, forming again a zigzag chain; (C) Si_{Ga} atoms on-surface and Si_{As} subsurface, forming a row of $\text{Si}_{\text{Ga}}-\text{Si}_{\text{As}}$ (001)-oriented pairs; and (D) the complementary configuration with Si_{As} atoms on the surface and Si_{Ga} in subsurface. We show here as an example the results for configuration B. In Fig. 2 we report a ball and stick model of this structure, together with the two corresponding simulated STM images. We can see a very bright signal at negative bias voltages that is strongly attenuated at positive voltages. With lower resolution, the bright signal would appear as a line 1–1.5 nm wide; that is, of dimension comparable with those reported in Ref. 1. The charge state has little influence on the XSTM image (results not shown here). The other cases (A, C, and D) are similar to this, apart from the negative charge state of C and D, where a weakly bright signal remains also at positive voltages.

Coming to a Si single monolayer uniformly distributed over two adjacent (001) atomic layers—that is, with one substitutional impurity every two atoms—the overall features

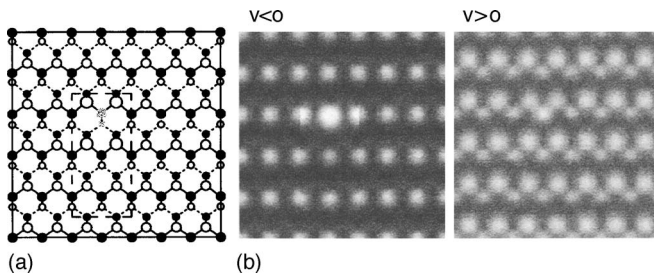


FIG. 3. Isolated Si_{Ga}-Si_{As} pair exposed on (110) GaAs surface: Si_{As} on surface, Si_{Ga} subsurface (see Fig. 2 caption). In this figure the supercell is not repeated in the [110] and [001] directions.

found for the full bilayer also show in this case. In particular, the bright/attenuated contrast at negative/positive bias remains a characteristic feature also in configurations with a reduced local concentration of Si dopants, which are more likely to occur in real samples.

In order to better characterize the microscopic origin of this feature, we have simulated the XSTM images of the point dipoles that would result from isolated Si_{Ga}-Si_{As} pairs on the exposed surface. In Fig. 3 we show the case in which the donor and the acceptor lie in different on-surface and subsurface atomic layers. Note that the bright spots ≈ 0.3 nm wide at negative bias visible in this figure correspond to an individual impurity confined to the exposed surface, whereas in the previous cases (A-D) they were representative of an entire doping layer shadowed by the surface spot. The resulting image is much less contrasted than that corresponding to the full bilayer, but the overall appearance is similar. The different contrast between the images of the full bilayer and those of the isolated dipole indicate, therefore, that the Si atoms in the inner layers also contribute to the modification of the local density of states and of the XSTM image.

Summarizing, we have shown that self-compensating donor-acceptor layer configurations of Si dopants are characterized by bright features at negative bias that are strongly attenuated by reversing it, in close resemblance with experimental images of Si-doping layers embedded in GaAs samples. We believe that in spite of the uncertainties due to several factors (tunneling voltage, nature and shape of the tip in case of experiments, specific technical details of the numerical simulations) not fully under control, our findings provide a qualitatively correct picture of the microscopic mechanism responsible for the observed images, thus point-

ing to the value of first-principles simulations as a tool for the characterization of materials.

This work was supported, in part, by the Italian National Institute for the Physics of Matter (INFN) under the project PRA-XSTMS and the “Iniziativa Trasversale di Calcolo Parallelo.” We gratefully acknowledge useful discussions with A. Franciosi, S. Rubini, and M. Piccin from INFN-TASC National Laboratory in Trieste. One of us (M. P.) also acknowledges support for computational facilities provided by the University of Trieste under the agreement with the Consorzio Interuniversitario CINECA.

¹S. Modesti, R. Duca, P. Finetti, G. Ceballos, M. Piccin, S. Rubini, and A. Franciosi, *Phys. Rev. Lett.* **92**, 086104 (2004).

²Ph. Ebert, *Surf. Sci. Rep.* **33**, 121 (1999), and references therein.

³R. M. Feenstra, *Phys. Rev. B* **50**, 4561 (1994).

⁴J. Wang, T. A. Arias, J. D. Joannopoulos, G. W. Turner, and O. L. Alerhand, *Phys. Rev. B* **47**, 10326 (1993).

⁵G. Lengel, R. Wilkins, G. Brown, M. Weimer, J. Gryko, and R. E. Allen, *Phys. Rev. Lett.* **72**, 836 (1994).

⁶R. B. Capaz, K. Cho, and J. D. Joannopoulos, *Phys. Rev. Lett.* **75**, 1811 (1995).

⁷S. B. Zhang and A. Zunger, *Phys. Rev. Lett.* **77**, 119 (1996).

⁸H. Kim and J. R. Chelikowsky, *Phys. Rev. Lett.* **77**, 1063 (1996); *ibid.* **409**, 435 (1998).

⁹Ph. Ebert, P. Quadbeck, K. Urban, B. Henninger, K. Horn, G. Schwarz, J. Neugebauer, and M. Scheffler, *Appl. Phys. Lett.* **79**, 2877 (2001).

¹⁰M. Peressi, S. Baroni, R. Resta, and A. Baldereschi, *Phys. Rev. B* **43**, 7347 (1991).

¹¹G. Biasol, L. Sorba, G. Bratina, R. Nicolini, A. Franciosi, M. Peressi, S. Baroni, R. Resta, and A. Baldereschi, *Phys. Rev. Lett.* **69**, 1283 (1992).

¹²The (110) slab geometry is obtained by applying periodic boundary conditions in the (110), (110) and (001) directions. The former is used to describe repeated parallel slabs (containing nine atomic planes perpendicular to the (110) direction in our case), separated by a vacuum region (of about 12 Å in our case) large enough to guarantee a sufficient separation of two adjacent surfaces. The last two periodic boundary conditions are used to describe the infinite surface; the surface unit cell for the doped configurations has to be large enough (up to 20 atoms in the present cases) in order to guarantee a sufficient separation between periodic images of the impurities.

¹³S. Baroni, A. Dal Corso, S. de Gironcoli, and P. Giannozzi, <http://www.pwscf.org>. We use pseudopotentials with the Perdew-Zunger exchange-correlation functional, plane-wave basis set expanded up to a kinetic energy cutoff of 14 Ry, special-point technique ($6 \times 4 \times 1$ mesh for self-consistent calculations and a $12 \times 8 \times 2$ mesh for non-self-consistent calculations) and Gaussian broadening (smearing parameter equal to 0.01 Ry) for Brillouin-zone integrations. Calculations are performed at 0 K.

¹⁴J. Tersoff and D. R. Hamann, *Phys. Rev. Lett.* **50**, 1998 (1983); *Phys. Rev. B* **31**, 805 (1985).